

## Charge-state trapping at a conducting polymer–redox ion-exchanger interface — a bilayer electrode

Duke Orata \*, Benson Kariuki

*Department of Chemistry, University of Nairobi, P.O. Box 30197, Nairobi, Kenya*

Received 25 May 1995; revised version accepted 25 September 1995

### Abstract

The results presented in this paper highlight the use of Amberlite, a commercial cation-exchange resin as a material for electrode modification.

We also show that when a redox centre is attached to the cation-exchange resin and an interface developed between it and a conducting polymer (polyaniline), electrochemical features characteristic of bilayer electrodes such as charge ‘trapping’ are observed

*Keywords:* Amberlite; Polyaniline; Charge ‘trapping’; Bilayer electrode

### 1. Introduction

The basic concept of solid-state electronics technology has always revolved on unidirectional flow of electrons across an interface between two substances, typically semiconductor materials. In general, carrier depletion or surface charge layers in semiconductor material leads to potential gradients which results in unidirectional electron flow [1–10].

Studies on charge rectification at electrolyte solution/semiconductor interface has been of particular interest in photoelectrochemistry [2]. In the recent past, two layer film assemblies have been studied. These have mostly centred on polymeric forms of complexes such as  $[\text{Ru}(2,2'\text{-bipyridine})_2\text{-}(4\text{-vinylpyridine})_2\text{Cl}](\text{ClO}_4)$ ,  $[\text{Ru}(2,2'\text{-bipyridine})_2\text{-}(4\text{-vinylpyridine})_2](\text{ClO}_4)$ , poly(ben-

zyviologen silane), polyvinylidiquat, etc. [3].

Use of cation-exchangers as electrode modification materials is also gaining momentum especially given the fact that these electrodes find ready use in analysis.

These ion-exchange-derivatized electrodes have been used in the determination of ceftriaxone in aqueous humour and serum samples [11], study of electrochemically assisted metal uptake [12], copper speciation analysis [13], study of the voltammetric behaviour of thallium(III) [14], determination of trace metals [15], voltammetric determination of trace amounts of mercury [16] and the cathodic stripping of paraquat [17].

In this paper the two layer assembly consists of a conducting polymer — polyaniline — and an ion-exchange resin — Amberlite. The latter has a copper redox centre attached to it. The attachment of the copper redox centre has been achieved by simultaneous exchange (SE) and

\* Corresponding author.

physical adsorption (PA), methods which have been discussed in detail in the paper. Thus in this paper, we will demonstrate the versatility of Amberlite as a material for electrode modification and that, when a redox centre is attached to the Amberlite, the resultant two-layer assembly formed with the conducting polymer — polyaniline — displays electrochemical features characteristic of bilayer electrodes.

## 2. Experimental section

All chemical reagents were used as received without further purification. The aniline was triply distilled until a colourless liquid was obtained. The commercial ion-exchange resin (Amberlite CG-50 BDH) was used as received. It consists of a cross-linked poly-(acrylic-acid-divinylbenzene) matrix. This resin has weakly acidic active group —COOH. The cation-exchange resin has a mesh size (U.S.S.) ranging from 100–200; a wet density (g/ml) of about 0.7 on rehydration; exchange capacities of 3.5 meq/ml (wet) and 10.0 meq/ml (dry); and a pH range of 5–14.

The cyclical potential scans were obtained using a PAR model 173 potentiostat/Galvano-

stat in conjunction with a model 175 Universal Programmer. The output signal was fed into a PAR RE 0089 X-Y recorder.

The X-ray fluorescence (XRF) spectral measurements were carried out on an IBM PC with the AXIL programme for spectrum analysis using QAES(75) for quantitative analysis using the algorithms based on fundamental parameter technique.

Analyses involving bare carbon electrode surface area,  $0.38 \text{ cm}^2$ , were conducted after the latter was polished on a felt polishing cloth using alumina. Amberlite modification of the electrode surface was achieved by mixing about 40 mg of Amberlite with 0.05 ml of a nonelectroactive binder (Henkel, k Ltd). The surface area of the Amberlite-modified electrode was approximately  $0.64 \text{ cm}^2$  and had a thickness of approximately 0.16 mm.

The reference and auxiliary electrodes used were saturated calomel electrode and platinum wire, respectively.

## 3. Results and discussion

In the set of experiments to be discussed, the key objective was to study the electrochemical

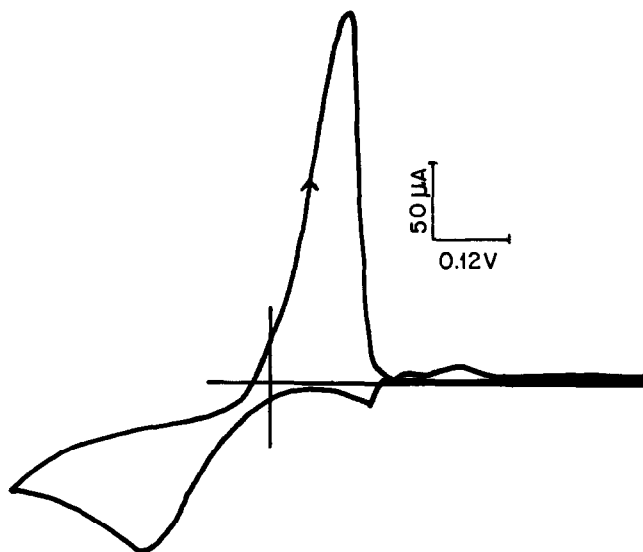


Fig. 1. Cyclic voltammogram of copper on an unmodified carbon electrode on cycling the potential in the range  $-0.3 \text{ V}$  to  $0.6 \text{ V}$  at a scan rate of  $20 \text{ mV/s}$  in a solution containing  $0.1 \text{ M}$  sulphuric acid and  $0.01 \text{ M}$  copper sulphate.

interaction between two redox centres whose formal potentials are close. In our case, the redox centres were those of copper and polyaniline.

The copper redox centre was to be attached to a host matrix, in this case Amberlite, which is a cation exchanger. We anticipated the formation of a bilayer especially when polyaniline is electrodeposited on a copper containing Amberlite host matrix. We started our electrochemical analysis by studying the copper redox process on a bare carbon electrode.

The carbon graphite working electrode was dipped into a solution containing 0.01 M copper sulphate and 0.1 M sulphuric acid. The potential was cycled from  $-0.3$  V to  $0.6$  V, at a scan rate of  $20$  mV/s. The cyclic voltammogram obtained, is characterized by an oxidation peak at  $0.12$  V and a reduction peak at  $-0.12$  V (see Fig. 1). On continued cycling, both the oxidative and reductive peak currents remain relatively constant.

We observe from the cyclic voltammogram that the difference between anodic and cathodic charge is approximately 17%. This value has been computed based on the difference between the areas under the cyclic voltammograms in comparison to the total area.

The next set of experiments involved modification of the working electrode surface using Amberlite containing copper redox centres. Attachment of copper redox centres on the Amberlite was achieved by 'simultaneous' exchange and 'physical' adsorption.

In simultaneous exchange, the Amberlite-modified electrode was allowed to exchange the copper during the electrochemical experiment, whilst physical adsorption entailed soaking the Amberlite in a solution containing copper sulphate for 24 hours, with continued stirring, followed by drying of the Amberlite at  $25^{\circ}\text{C}$  before being used to modify the working electrode surface.

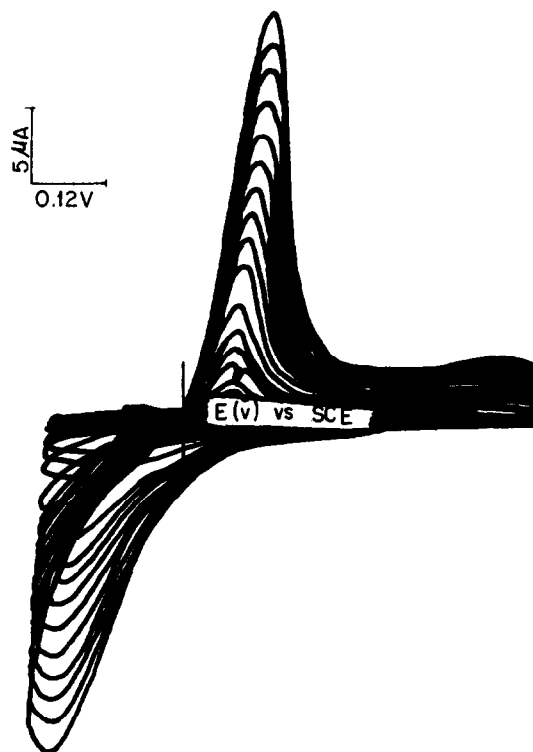


Fig. 2. Cyclic voltammograms of copper on an Amberlite-modified electrode on cycling the potential in the range  $-0.3$  V to  $0.6$  V at a scan rate of  $20$  mV/s in a solution containing  $0.1$  M sulphuric acid and  $0.01$  M copper sulphate.

The cyclic voltammetric response obtained from the Amberlite-modified electrode during the cycling of potential in the range  $-0.3$  V to  $0.6$  V in a solution of  $0.1$  M sulphuric acid and  $0.01$  M copper sulphate (for simultaneous exchange case) displayed the same electrochemical features as those exhibited in the bare carbon case, only that now the oxidation peak potential occurred at  $0.1$  V, indicating a shift towards neg-

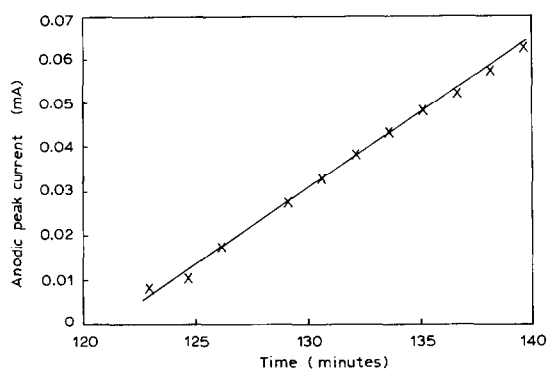


Fig. 3. A plot of oxidation peak current versus time for copper on an Amberlite-modified electrode on cycling the potential in the range  $-0.3$  V to  $0.6$  V at a scan rate of  $20$  mV/s in a solution containing  $0.1$  M sulphuric acid and  $0.01$  M copper sulphate.

ative potentials of approximately  $20$  mV. The shift probably has no electrochemical significance other than, being due to  $iR$  drop in the electrode (see Fig. 2). A plot of the oxidative peak current versus time (see Fig. 3) yielded non-linear plots for different electrode samples under the same experimental conditions. The slopes had a value of approximately  $2.1 \times 10^{-3}$  mA/min. Similar patterns were observed for plots involving the cathodic peak current. It is important to mention that the increase in the peak currents is probably due simply to copper getting greater access to the underlying electrode, a fact verified by considering the reversibility of the process. The anodic and cathodic peaks increased with each subsequent cycle. The general shape of the voltammogram still resembled that seen in Fig. 2.

The next set of experiments involved electrodes modified using copper-loaded Amberlite. These electrodes were dipped into a solution containing  $1$  M sulphuric acid (no copper sulphate) and the potential cycled from  $-0.3$  V to  $0.8$  V at a scan rate of  $20$  mV/s, we obtained the cyclic voltammogram shown in Fig. 4. The anodic and cathodic peaks increased with each

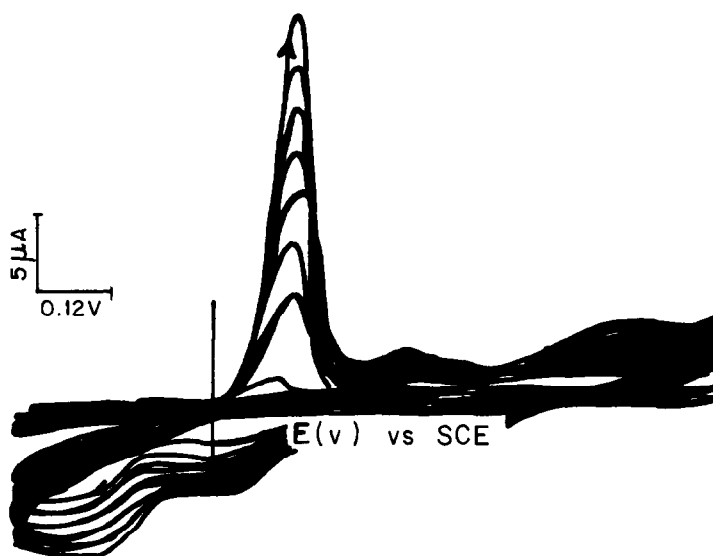


Fig. 4. Cyclic voltammograms obtained from a copper-loaded Amberlite-modified (by physical adsorption) electrode on cycling the potential in the range  $-0.3$  V to  $0.8$  V at a scan rate of  $20$  mV/s in  $1$  M sulphuric acid.

subsequent cycle. The copper oxidation peak occurs at 0.08 V. In all cases studied, we obtained linear plots for anodic versus cathodic peak current. Suggesting a high redox efficiency, i.e. for every incremental increase in the anodic peak

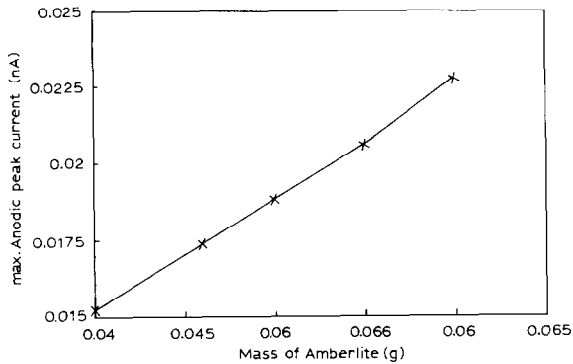


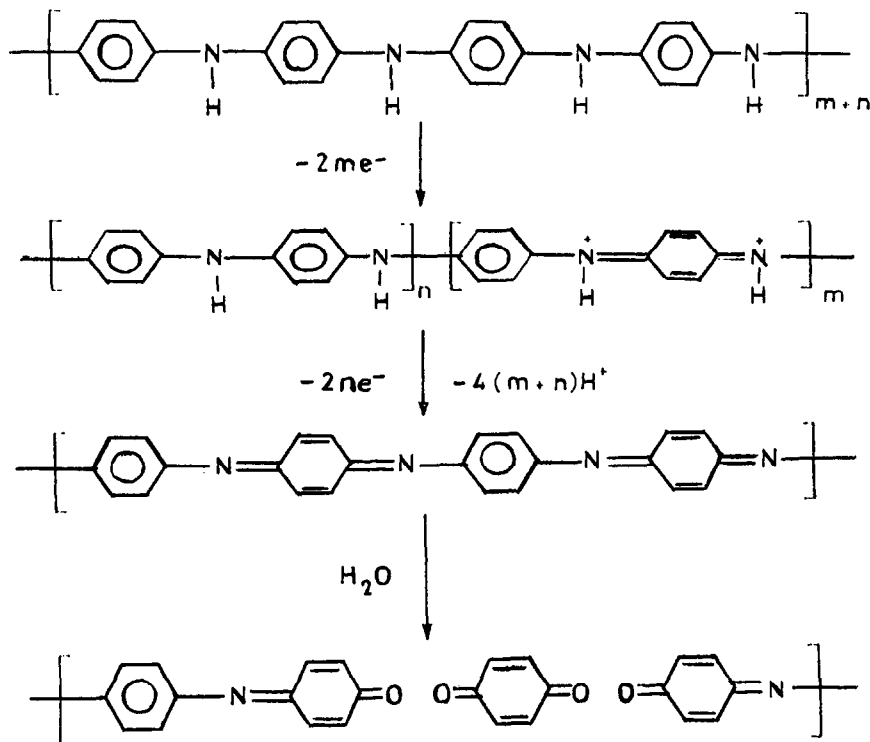
Fig. 5. A plot of maximum anodic peak current versus amount of copper-loaded Amberlite (by physical adsorption) used in the electrode modification on dipping the electrode in 1 M sulphuric acid and cycling the potential in the range  $-0.3$  to  $0.8$  V at a scan rate of  $20$  mV/s.

current, we have a corresponding increase in the cathodic peak current.

The next set of experiments involved attempts to relate the maximum anodic peak current on continuous potential cycling to the amount of copper-loaded Amberlite used in electrode modification. This was done by dipping a copper-loaded Amberlite-modified electrode in  $1.0$  M sulphuric acid solution and cycling the potential in the range  $-0.3$  V to  $0.8$  V. The Amberlite used in the analysis were all from the same sample of Amberlite soaked in the copper sulphate solution.

Several such experiments were repeated and a plot of the maximum anodic peak current versus mass of Amberlite used in the electrode modification made (see Fig. 5). The plot obtained was then used as a calibration curve mass of Amberlite used in the electrode modification.

In one instance the value of maximum peak current obtained was  $0.011$  mA instead of the expected value of  $0.012$  mA. The error can be at-



tributed to the difference in surface morphology i.e., Amberlite packing at the electrode surface or partly due to leaching of the electroactive species, since these experiments involved exposure of the electrode to the solution for long periods of time.

We calculated the surface coverage of the electroactive copper from the slope of a plot of  $\Gamma_{\text{Cu}}$  versus amount of Amberlite used in electrode preparation and obtained a value of  $1.5 \times 10^{-6}$  grams of copper per gram of Amberlite based on the equation

$$\Gamma_{\text{Cu}} \times \text{mol. weight of CuSO}_4 \times \text{electrode area}$$

Thus electroactive copper weighs 0.00024% of the total weight of the electrode modification material.

When samples of Amberlite soaked in copper sulphate solutions were subjected to X-ray fluorescence analysis (XRF) to determine the amount of copper, a value of  $1.49 \times 10^{-3}$  grams of copper per gram of Amberlite was obtained (see Table 1). Thus, the amount of nonelectroactive copper in Amberlite was  $1.487 \times 10^{-3}$  grams. Electroactive copper, therefore constitutes approximately 0.16% of the copper contained in the Amberlite. This suggests that most of the copper in the Amberlite is not electroactive. This low value of  $\Gamma_{\text{Cu}}$  (electroactive) can be attributed to the fact that the electroactive copper are those adsorbed onto the surfaces of the cation exchanger or on sites resulting from defects, i.e. holes.

Table 1  
Elemental composition of Amberlite soaked in 0.01 M copper sulphate and 0.1 M sulphuric acid for 24 hours

Element	Concentration $\times 10^3$ (g/g)
P	113.10
S	21.23
Cl	3.43
K	2.87
Sn	50.00
Ca	27.85
Cu	1.49
Fe	0.54

In the next set of experiments we electrodeposited the conducting polymer — polyaniline — on Amberlite-modified electrode. We started by cycling the potential of an Amberlite- (no copper-) modified electrode from  $-0.3$  V to  $0.8$  V at a scan rate of  $20$  mV/s, in a solution containing  $1.0$  M sulphuric acid and  $0.1$  M aniline. The oxidation peak occurred at  $0.19$  V. It is surprising that we do not have a dramatic difference in the oxidation potentials of polyaniline electrodeposited on an Amberlite electrode as compared to that electrodeposited on a bare carbon electrode, since we had expected electrostatic interaction between cationic sites generated on oxidation of polyaniline (see Scheme 1) and those of the anionic sites (weakly acidic group such as  $-\text{COO}-$ ) found in the cation-exchange resin to

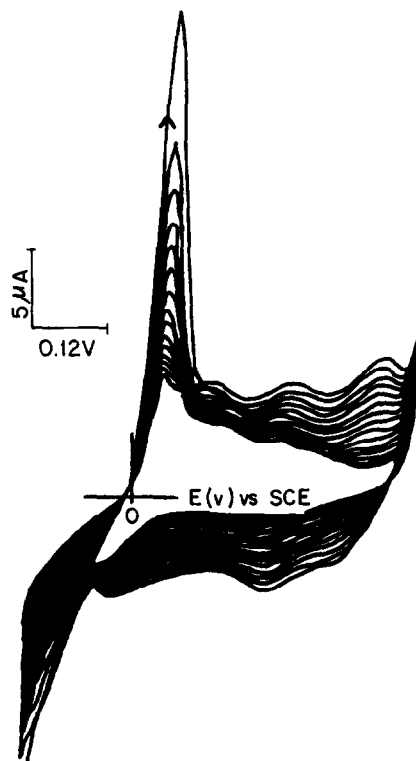


Fig. 6. Cyclic voltammograms obtained on transferring a copper-loaded Amberlite (by simultaneous exchange) into a solution containing  $1$  M sulphuric acid and  $0.1$  M aniline and cycling the potential in the range  $-0.3$  to  $0.8$  V at a scan rate of  $20$  mV/s.

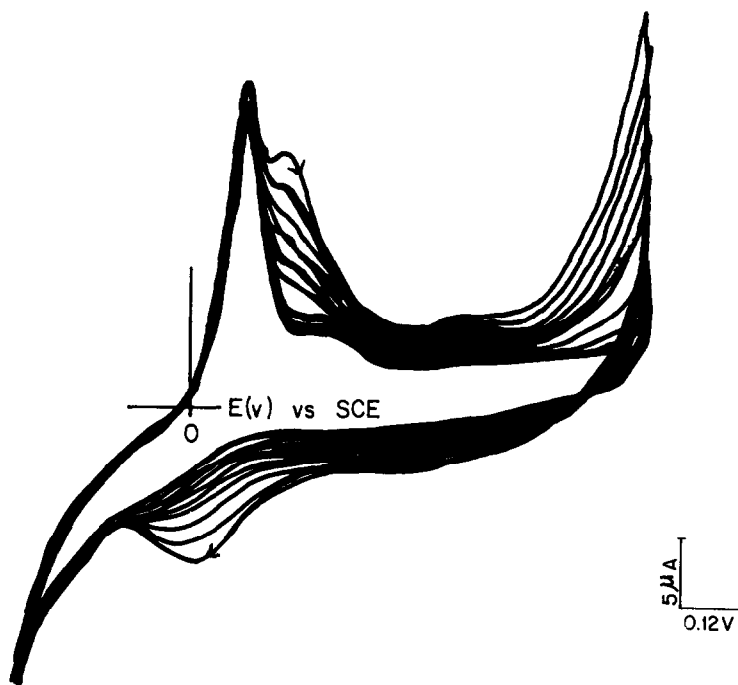


Fig. 7. Cyclic voltammograms obtained on dipping a copper-loaded Amberlite-modified (by physical adsorption) electrode in a solution containing 1 M sulphuric acid and 0.1 M aniline and cycling the potential in the range  $-0.3$  to  $0.8$  V at  $20$  mV/s.

affect the redox potentials. The absence of electrostatic interference between polyaniline and the cation-exchange resin is probably a veiled pointer to the two units being distinctly separate, i.e. bilayer arrangement.

When a similar experiment was repeated but this time using a copper-loaded Amberlite (in a solution containing 1 M sulphuric acid and 0.1 M aniline) as the electrode modification material, we obtained different results. The results obtained also depended very strongly on the mode of attachment of the copper redox centre on the Amberlite i.e., simultaneous exchange (SE) or physical adsorption (PA). Experiments conducted on the SE-Amberlite electrode revealed copper oxidation/reduction peaks which were decreasing while three other oxidation peaks were building up at  $0.19$  V,  $0.36$  V and  $0.71$  V (see Fig. 6).

The oxidation peak at  $0.19$  V results from the polyaniline oxidation process, while those at  $0.36$  V and  $0.71$  V are attributed to quinone–quinone

imine derivatives, characteristic of polyaniline at very positive potentials [10].

When similar experiments were conducted on the PA-Amberlite electrode, we observed the polyaniline redox peak starting as a shoulder off the copper oxidation peak, gradually developing into a well-defined peak (see Fig. 7). The double humped copper–polyaniline peak finally merges into one distinct peak. The peak potential of this new peak corresponds to that characteristically observed for polyaniline (see Fig. 8).

The interesting thing is that at some stage during the electrochemical process, the copper redox state appears ‘trapped’, i.e. invariant, as the polyaniline redox peaks develops. This status is maintained throughout until when the polyaniline peak becomes dominant. This charge trapping is a further pointer to a possible bilayer formation [3].

In this arrangement we can treat PA-Amberlite as the inner film and the polyaniline as the outer film. The current controlling

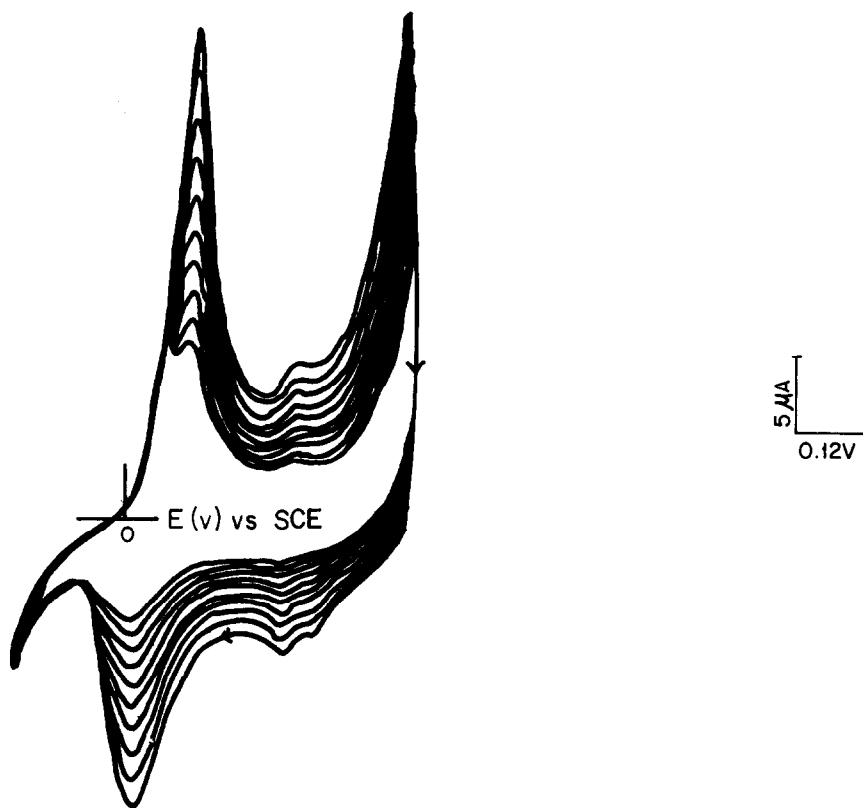


Fig. 8. Cyclic voltammograms obtained after the merging of the copper and polyaniline oxidation peaks.

steps will include oxidation of copper redox sites, electrochemical charge transfer through the PA-Amberlite and polyaniline film, and finally electron transfer between the redox centres, i.e. PA-Amberlite and polyaniline. The rate determining step will be electron transfer between the PA-Amberlite and polyaniline redox centres, as the other processes are relatively fast, i.e. the peak currents are proportional to scan rate implying that charge transport is fairly rapid. We cannot use expressions similar to those used in Ref. [3], as the redox system in this case is quasi-reversible.

#### 4. Conclusion

The results presented highlight the significance of electrode modification in bringing out salient electrochemical features which cannot be observed on unmodified electrodes.

Even though we observe a trapped charge state, it is important to mention that this bilayer phenomena will have to be investigated using different redox systems and try to establish how reversibility of the system affects the various electrochemical parameters encountered in bilayer analysis.

#### References

- [1] H.D. Abruna, P. Denisevich, M. Umana, T.J. Meyer and R.W. Murray, *J. Am. Chem. Soc.*, 103 (1981) 1.
- [2] A.J. Nozik, *Annu. Rev. Phys. Chem.*, 29 (1978) 189.
- [3] R.W. Murray, P. Denisevich and K.W. William, *J. Am. Chem. Soc.*, 103 (1981) 4727–4737.
- [4] (a) N. Oyama, K. Shigehara and F.C. Anson, *Inorg. Chem.*, 102 (1981) 518;  
 (b) F.C. Degrand and L.L. Miller, *J. Am. Chem. Soc.*, 102 (1980) 5728;  
 (c) F.C. Anson and N. Oyama, *J. Electrochem. Soc.*, 127 (1980) 640;  
 (d) A.J. Bard and P.J. Pearce, *J. Electroanal. Chem.*, 114 (1980) 89.



- [5] R.W. Murray and P.J. Danm, *Electroanal. Chem.*, 103 (1979) 289.
- [6] D. Rolison, R.W. Murray, J.R. Lenhard and P.J. Daum, *J. Am. Chem. Soc.*, 102 (1980) 4649.
- [7] R.W. Murray, R. Lann, M. Umana, F.A. Schultz and R. Nowak, *Anal. Chem.*, 52 (1980) 315.
- [8] R.W. Murray and P.J. Daum, *J. Phys. Chem.*, 85 (1981) 389.
- [9] Y.L. Jim and C.T. Thiam, *J. Electrochem. Soc.*, 137 (1990) 1402.
- [10] D. Orata and D.A. Buttry, *J. Am. Chem. Soc.*, 109 (1987) 3514 and references therein.
- [11] S. Altinoz, D. Ozer, A. Temizer and N. Yuksel, *Analyst*, 119(7) (1994) 1575.
- [12] S. Wu-w, M.S. Uddin, H. Chi and K. Hidajat, *J. App. Electrochem.*, 24(6) (1994) 548.
- [13] R. Agraz, M.T. Sevilla and L. Hernandez, *Anal. Chim. Acta.*, 283(1) (1993) 650.
- [14] W. Diewald, K. Kalcher, C. Neuhold, X. Cai and R.J. Magee, *Anal. Chim. Acta.*, 273(1–2) (1993) 237.
- [15] R. Agraz, Sevilla, M.T. and Hernandez, L, *Anal. Chim. Acta.*, 273(1–2) (1993) 205.
- [16] X. Cai, K. Kalcher, W. Diewald, C. Newhold and R.J. Magee, *Fres. J. Anal. Chem.*, 345(1) (1993) 25.
- [17] E. Alvarez, M.T. Sevilla, J.M. Pinnilla and L. Hernandez, *Anal. Chim. Acta.*, 260(1) (1992) 19.